The exopolysaccharide–eDNA interaction modulates 3D architecture of Bacillus subtilis biofilm

Na Peng

Huazhong Agriculture University

Peng Cai

Monika Mortimer

University of California

Yichao Wu

Huazhong Agriculture University

Chunhui Gao

Huazhong Agriculture University

Qiaoyun Huang

Huazhong Agriculture University

Research article

Keywords: extracellular DNA (eDNA), exopolysaccharides (EPS), Bacillus subtilis, biofilm formation

---

Abstract

Background Bacterial biofilms are a surface-adherent microbial community in which individual cells are surrounded by a self-produced extracellular matrix of polysaccharides, extracellular DNA (eDNA) and proteins. Interactions among matrix components within the biofilms are responsible for creating an adaptable structure during biofilm development. However, it is unclear how the interaction among matrix components contributes to the construction of the three-dimensional (3D) biofilm architecture.

Results DNase I treatment could significantly inhibit B. subtilis biofilm formation in early phases. Confocal laser scanning microscopy (CLSM) and image analysis revealed that eDNA was cooperative with EPS in early stages of B. subtilis biofilm development, while EPS played a major structural role in the later stages. In addition, deletion of EPS production gene epsG in B. subtilis SBE1 resulted in loss of the interaction between EPS and eDNA, and reduction of biofilm biomass in pellicles at air-liquid interface. The physical interaction between these two essential biofilm matrix components was confirmed by isothermal titration calorimetry (ITC).

Conclusions The biofilm 3D structures become interconnected through surrounding eDNA and EPS. eDNA interacts with EPS in the early phases of biofilm development, while EPS mainly participates in the maturation of biofilm. The findings of this study provide better understanding of the role of interaction between eDNA and EPS in shaping the biofilm 3D matrix structure and biofilm formation.

Background

Bacterial biofilms are heterogeneous communities that exhibit a remarkable degree of spatiotemporal organization [1–3]. The spatial architecture of multicellular communities depends on the production of extracellular matrix, mainly composed of polysaccharides, proteins, and extracellular DNA (eDNA) [4, 5]. eDNA as an important matrix component in biofilms [5, 6], can be used by bacteria for several vital functions, such as structural component of biofilms [7], nutrient source [8], and a gene pool for horizontal gene transfer (HGT) [9]. The significance of eDNA in biofilm formation has been studied in Pseudomonas aeruginosa [6], Staphylococcus epidermidis [10], Streptococcus pneumoniae [11] and Vibrio cholerae [12]. In these studies, young biofilms were easily disturbed by DNase I treatment, but this was no longer effective in aged biofilms. This loss of sensitivity to DNase I treatment suggests that either other extracellular matrix components complement or replace eDNA functions within the mature biofilms, or that eDNA is shielded from enzymatic degradation when bound to other biofilm components.

Exopolysaccharide (EPS) is one of the major extracellular biofilm matrixes [13, 14, 15]. Interactions between EPS and eDNA have been investigated in some bacterial biofilms. In Streptococcus mutans biofilm, the interaction of eDNA with glucans forms filamentous structures which play an important role in the connection of bacterial cells [16]. In the case of P. aeruginosa, eDNA and exopolysaccharide Psl physically interact in biofilms to form the web of Psl–eDNA fibers, which functions as a skeleton facilitating bacterial adhesion and growth [17]. Meanwhile, Psl can interact with the genomic DNA from

human neutrophils or other strain S. aureus, implying that P. aeruginosa can utilize genomic DNA from other organisms to form its own community [17]. Therefore, eDNA–EPS interaction is important for the construction of biofilm architecture.

Bacillus subtilis, a Gram-positive bacterium, produces a variety of biologically active compounds with a broad spectrum of activities against plant pathogens [18–23]. Due to the role of B. subtilis as a biocontrol agent in agricultural settings, a growing number of studies has focused on the biofilm formation in natural and artificial conditions [18, 24–26]. The EPS is a key component in B. subtilis matrix that promotes cells binding together in structural biofilms [27]. It has been proposed that the eDNA release by dead cells during the process of cannibalism in B. subtilis 168, could be related with matrix development [28–31]. On the other hand, eDNA released from B. subtilis 3610 during stationary phase is not involved in biofilm establishment [32]. However, how eDNA interactions with EPS modulate B. subtilis biofilm formation processes and architecture constructions is less known.

This study focused on elucidating the role of the eDNA in (1) the construction of the B. subtilis biofilm 3D architecture, and (2) interaction with EPS during biofilm formation. Here we used CLSM and image analysis to investigate the role of eDNA during B. subtilis SBE1 biofilm structure construction. And ΔepsG strain (deletion of one of EPS production gene) was used to examine the role of EPS and its interaction with eDNA during biofilm development. To better understand the interactions of EPS and eDNA, isothermal titration calorimetry (ITC) was used to study the thermodynamics of these two molecules interactions. The results of this work contribute to the understanding of interactions between B. subtilis biofilm matrix components and the development of adaptable biofilm structure over time.

Methods

Soil isolate of *Bacillus subtilis* SBE1, which is an "undomesticated" strain, was obtained from the State Key Laboratory of Agricultural Microbiology, Huazhong Agriculture University (Wuhan, China). This strain has been deposited in China Center for Type Culture Collection (CCTCC), and the accession number is CCTCC AB 2018210. The whole genome sequences have been deposited at DDBJ/ENA/GenBank under accession QPGT01000000. Phylogenetic tree and gene family analysis of *B. subtilis* is presented in Fig. S1. Bacterial strains were cultured in lysogeny broth (LB) (10 g of tryptone, 5 g of yeast extract, and 10 g of NaCl per liter of broth) at 37 °C. The strains, plasmids, or primers used in this study are shown in Table S1.

Furthermore, *epsG* mutant was generated by using long flanking homology PCR [33]. Constructs generated were inserted by double recombination into integration sites (*epsG*) in the genome of *B. subtilis* by inducing natural competence. Primers used are listed in Table S1. They were cloned in pDG780, a vector carried *kan* gene. Constructions were transferred to *B. subtilis* SBE1 by electroporation transformation. The relative amounts of bacterial cell-associated carbohydrate were estimated by Phenol-sulfuric acid method (see details at supplementary material).

DNase I treatment of biofilm

The role of eDNA in *B. subtilis* biofilm formation was investigated by adding DNase I (100 Kunitz units per mL) (Sigma-Aldrich, Steinheim, Germany) to the inoculum to degrade eDNA produced during growth. Briefly, after incubation (see Bacterial Culture above), bacteria were resuspended in minimal salts glycerol glutamate (MSgg) medium [34], and diluted to an OD_{600} of 0.05. Next, 200 μL of the bacterial suspension was added to each well of a 96-well microtiter plate and incubated at 37 °C without shaking. After 3, 6, 12, 24, 48, and 72 h, the supernatant from each well was removed, then the biofilms (pellicles) were washed twice with 1 mL sterile 0.9% NaCl. And 10 μL of DNase I (final concentration: 100 Kunitz units per mL) was either added at the beginning of the experiment or after the biofilm had established. The biofilm biomass was quantified using crystal violet assays [34]. For each analysis, 1 % w/v crystal violet solution (200 μL) was added to eight replicate wells, incubated for 10 min, and rinsed twice with 200 μL sterile distilled water. The crystal violet in the residual biofilm was dissolved in 200 μL absolute ethanol. Then, OD at 595 nm was measured using a plate reader (PerkinElmer, Waltham, USA).

Atomic Force Microscopy (AFM)

The topography of the biofilms with and without DNase I treatment (12 h) was investigated at room temperature (25 °C) using a MultiMode 8 AFM with a NanoScope V controller (Bruker). The scanning modes used were: 1) the ScanAsyst mode using ScanAsyst-Air cantilevers with 0.4 N m^{-1} nominal spring constant (Bruker); 2) the tapping mode using RTESP cantilevers with 40 N m^{-1} nominal spring constant (Bruker) [35]. A scan size of 10×10 μm was used. Images were processed and analysed using NanoScope Analysis (Bruker).

Confocal Image acquisition and analysis

The air-liquid interface biofilms were grown in 20mm bottom cell culture dish (Nest). DNase I (100 Kunitz units per mL) was added to glass chamber during inoculation. For CLSM observation, buffer was gently removed from glass chambers to allow the pellicles to drop onto glass bottom [36]. The biofilms were stained with Live/Dead ^{TM} Bacterial viability Kit (Bac Light ^{TM}, Molecular Probes, Invitrogen). The arrangement of the biofilm matrix was determined by direct incorporation of fluorescent labels during synthesis of the exopolysaccharide (EPS) and eDNA matrix, which allowed the examination of the 3D structure within intact biofilms [15, 37]. The labeling of EPS and eDNA matrix were done after biofilms were developed. Extracellular DNA in biofilms was labeled by TOTO-1 nucleic acid stain (cell impermeable, 514/533 nm; Molecular Probes) and PI nucleic acid stain (cell impermeable, 535/615 nm; Molecular Probes). The exopolysaccharide matrix was labeled by ConA (α-polysaccharides) (590/617 nm; Molecular Probes) [38]. The bacteria in biofilms were labeled by SYTO 9 nucleic acid stain (cell permeable, 485/535 nm; Molecular Probes) and SYTO 60 nucleic acid stain (cell permeable, 652/678 nm; Molecular Probes). The imaging was performed using Olympus FV 1000 monophoton laser scanning microscope (Olympus, Tokyo, Japan) equipped with 40× (0.95 numerical aperture) objective lens.

The confocal images were analyzed by using software to visualize and quantify the bacterial cells, EPS and eDNA within intact biofilms. Imaris 7.4.2 (Bitplane AG, Zurich, Switzerland) was used to rebuild each

structural component (bacteria, EPS and eDNA) within the biofilms for visualizing the 3D architecture and morphology. Quantitative characterization of each structural component within 3D biofilm images was done as reported previously [15, 39]. The images were imported to JACoP (Fabrice P. Cordelieres, Institut Curies, Orsay, France), a plugin for the Image J software (40). Then Pearson's coefficient (PC), the thresholded Mander's coefficients tM_1 and tM_2 were calculated as described previously [33, 48].

DNA purification and preparation of EPS extract

Genomic DNA of *B. subtilis* SBE1(final concertation: 0.003 mol/L), *B. subtilis* 3610 (0.005 mol/L), *Shewanella oneidensis* MR1 (0.01 mol/L) and *Pseudomonas putida* KT2440 (0.07 mol/L) was extracted by using Wizard Genomic DNA Purification Kits (Promega). EPS was extracted from batch culture of *B. subtilis* SBE1 as previously described [7]. To remove the DNA, crude EPS was treated with both enzymes, the DNase I (3 h at 37°C) was added 1 h before the proteinase K (3 h at 60°C) was added. The enzymes were used at a final concentration of 100 µg mL^{-1}.

Isothermal titration calorimetry (ITC)

Enthalpy changes (ΔH) of the interaction between DNA and EPS were determined by isothermal calorimetry using a NANO ITC 2G (TA Instruments, USA). EPS and genomic DNA were dissolved into 0.01 M PBS (pH 7.4). EPS (2.25 mg mL^{-1}) was dispensed into the microcalorimetric cell (volume 1.3 mL), and the DNA solution was filled into the syringe compartment (volume 250 µL). DNA was titrated in 10 µL portions (3.14 µL for the first injection) into the EPS containing cell under constant stirring, and the heat of reaction was plotted versus time. All measurements were performed at 25 °C. Data was analyzed by using NANOANALYZE software [41].

Statistical analysis

Data were basically described by means and respective standard deviations (SD). P-values were acquired using analysis of variance (ANOVA) followed by Tuckey's multiple comparisons test to evaluate statistical significance using SPSS 17.0 software. Differences were regarded as statistically significant when $p < 0.05$.

Results And Discussions

The role of eDNA in the construction of *B. subtilis* SBE1 biofilm 3D architecture

In order to understand the eDNA's contribution to the biofilm formation of *B. subtilis* SBE1, the impact of DNase I on biofilm formation was tested by using a static biofilm assay. Biofilms were grown either with or without DNase I (100 Kunitz units per mL) (Sigma-Aldrich, Steinheim, Germany) in the medium [42]. The formation of biofilms grown for 3, 6, and 12 hours with DNase I was clearly suppressed, compared with the untreated control, based on crystal violet assay (3 h, *P*=0.0020; 6 h, *P*=0.0003; 12 h, *P*=0.0000). In contrast, biofilms grown with DNase I for 24 and 48 hours were not significantly different from biofilms

grown without DNase I (Fig. 1A). DNaseI can not only inhibit the formation of biofilms but also disrupt established *B. subtilis* biofilms at the same time points (Fig. 1B). These results suggested the importance of eDNA in early *B. subtilis* SBE1 biofilm formation. The formed biofilm in 12-h in the presence of DNase I was further characterized using by atomic force microscopy (AFM) to measure the depth of the furrows generated (Fig. 2). Under the conditions in the absence of DNase I, furrows between cells were ~200 nm in depth (Fig. 2 A, B and E). In the presence of DNase I, the furrows of the expanding biofilm were significantly deeper (up to 400 nm) than those formed in the absence of DNase I (Fig. 2 C, D and E) (P<0.001), which suggested that the gaps between cells in biofilms may be filled with eDNA. These results are consistent with what has been reported for other species [42-44], indicating that eDNA may be an adhesion compound enabling cell-to-cell attachment, which stabilizes the biofilm [45].

To examine how eDNA functions as a cell-cell adhesin during biofilm development, the construction of eDNA matrix in 3D biofilm architecture was examined over time. The formation and the sequence of assembly of eDNA changed over time. After 12 h of biofilm development (Fig. 3A), the cells were densely packed in eDNA matrix, forming a 3D biofilm structure (termed the eDNA-microcolony complex, highlighted in Fig. 3A). After 24 h, the biofilm structures expanded in several dimensions with less eDNA-matrix enmeshed in and surrounded by the bacteria (Fig. 3B and 3C). Imaris analysis also showed that the content of eDNA in the biofilms substantially reduced after 24 h (Fig. 4B). These results suggested that other matrix components may complement eDNA as cell-cell adhesins when the biofilm becomes mature, or perhaps that eDNA in mature biofilms interacts with other biomolecules which can protect it from DNase degradation. It has been previously reported that cell-to-cell interactions occurred during the biofilm accumulation phase, which can be mediated by eDNA linking recycled cytoplasmic proteins of *S. aureus* [45]. Here in this study, eDNA was shown to promote biofilm formation (Fig. S2), and the cells within the biofilm were surrounded by eDNA at 12 h (Fig. 2), suggesting that eDNA may play an important role in cell-to-cell interconnection during early *B. subtilis* SBE1 biofilm formation. Later stages of *B. subtilis* SBE1 biofilms were less susceptible to DNase I-induced dispersal (Fig. 1b), indicating that another biofilm component (i.e. EPS) may replace eDNA within mature biofilm. It has also been reported that peptidoglycan, as an additional essential component, is required for DNA-dependent biofilm development in *Listeria monocytogenes* [46].

EPS and eDNA colocalization in *B. subtilis* SBE1 3D biofilms

The spatial assembly of EPS and eDNA at each developmental stage of wild type biofilms were examined at 12, 24 and 48 hours by CLSM (Fig. 4). Fig. 4Aa showed the 3D evolution of EPS-eDNA interaction over time. The cross-sectional images at each time point are shown in Fig. 4Ab-j. At the 12-hour time point, there was considerable eDNA in biofilms which connects bacteria with each other (Fig. 4A a (1)); at the 24-hour time point, most eDNA was peripherally localized and EPS was found to concentrate inside the biofilms (Fig. 4Aa (2)); at the 48-hour time point, eDNA and EPS covered the entire structure (Fig. 4Aa (3)).

This observation was supported by the quantitative colocalization analysis. As shown in Fig. 5, the Pearson's coefficient (PC) defines the quality of the linear relationship between the two signals. Manders'

coefficients is based on the Pearson's correlation coefficient with average intensity values being taken out of the mathematical expression. The thresholded Mander's coefficients were calculated setting the threshold to the estimated value of background instead of zero [47, 48]. The analysis of seven image stacks by these methods showed the complete colocalization of eDNA-EPS in wild type biofilms (Fig. 5A). The thresholded Mander's tM_1 (M1thr) indicated the fraction of eDNA (TOTO-1 signal, green) overlapping with EPS (ConA signal, orange), and tM_2 (M2thr) indicated the fraction of EPS overlapping eDNA. The PC (black bar) will tend to 0 when random noise is added to complete colocalizing structures. At 12 h, a wider distribution of eDNA was observed in intercellular space compared to EPS. Most of the EPS overlapped with the eDNA (M1thr < 0.5, M2thr > 0.5). At 24 h, most of the eDNA overlapped with the EPS (M1thr > 0.5, M2thr < 0.5). At 48 h, they were completely colocalized (M1thr > 0.5, M2thr > 0.5). This quantitative analysis was consistent with the CLSM observations, suggesting that eDNA was cooperative with EPS in early stages, while EPS might play a larger role in the later stages of *B. subtilis* SBE1 biofilm development.

Spatial assembly of EPS and eDNA in the epsG mutant *B. subtilis* SBE1 biofilms

To further confirm the spatial assembly of EPS and eDNA during the development of *B. subtilis* SBE1 biofilms, we constructed EPS defective mutant. It has been reported that the genes responsible for the production of EPS in *B. subtilis* are part of the *eps A-O* gene operon (*eps*) [27, 49-51]. And the deletion of the operon [27], *epsE* [51], *epsG* [50] or *epsH* [27] results in the lack of EPS production and thin pellicles [27, 52, 53]. *B. subtilis* SBE1 genome also contains homologous *epsA-O* genes (the genetic loci for *epsG* gene as follows: open reading frame Query_1049240 [*epsG*]). Fig. S2 showed that the *ΔepsG* mutant strain produced significantly less cell-associated EPS than wild type cells. The deletion of EPS production gene epsG in *B. subtilis* SBE1 also resulted in reduction of biofilm biomass in pellicles at air-liquid interface (Fig. S3). Then, the spatial assembly of EPS and eDNA at each developmental stage of *ΔepsG* mutant biofilms were also examined at 12, 24 and 48 hours by CLSM (Fig. 6). Quantitative image analysis showed that there was a substantial reduction in the contents of both eDNA and EPS in the biofilms of the *ΔepsG* strain compared to wild type *B. subtilis* SBE1 (Fig. 4 and 6). By using DNA dye TOTO-1 along with the EPS dye ConA, quantitative colocalization analysis showed that eDNA was colocalized with EPS in *B. subtilis* SBE1 pellicles but not in *ΔepsG* strain pellicles. In addition, the eDNA and EPS in *ΔepsG* mutant biofilms exhibited partial colocalization (12 h, 24 h) (M1thr < 0.5, M2thr < 0.5) (Fig. 5B). The colocalization of eDNA and EPS observed in native extracellular matrix provided evidences for direct interactions between eDNA and EPS in *B. subtilis* SBE1 biofilms. These results indicated that eDNA interacts with EPS in the early phases of biofilm development, while EPS participates in the maturation of biofilm. The transition of eDNA's role from initial construction of the 3D extracellular matrix to matrix micro-aggregation is similar to the transition mediated by eDNA and lipoteichoic acid (LTA) in biofilms of *Streptococcus mutants* [54].

The colocalization of eDNA and EPS in *B. subtilis* SBE1 pellicles suggested the potential physical interaction between these two components. Isothermal titration calorimetry (ITC) is an important technique to study the thermodynamics of molecule interactions. It has been used to study the molecular

interaction between protein and lipid polysaccharide (LPS) [55]. And we used ITC to confirm the interaction between DNA and EPS. Data in Figure S5A, B, C and D showed that the total heat for DNA from *B. subtilis* SBE1, *B. subtilis* 3610, *Shewanella oneidensis* MR1 and *Pseudomonas putida* KT2440 binding to EPS was 0.00015 ± 0.00002, 0.00024 ± 0.00003, 0.00095 ± 0.00005 and 0.00086 ± 0.00004 KJ (n = 3), respectively (Figure S4E). The calculated binding enthalpy (the binding heat per DNA molecule) of EPS were 222.72 ± 26.34, 162.77 ± 17.82, 338.46 ± 45.23 and 398.50 ± 38.67 kJ/mol (n = 3), respectively (Figure S4F), indicating that EPS can interact with DNA from diverse recourses.

Conclusions

eDNA and EPS, two essential matrix components of *B. subtilis* SBE1 biofilm, cooperate by physically interacting in bacterial biofilms. Over time, the biofilm 3D structures become interconnected through surrounding eDNA and EPS. eDNA interacts with EPS in the early phases of biofilm development, while EPS mainly participates in the maturation of biofilm. Based on our research, we proposed a model to describe how the eDNA-EPS interaction mediates the construction of the complex 3D biofilm architecture and establishes spatial heterogeneities in *B. subtilis* SBE1. Complex 3D biofilm forms in the following sequences: (1) initial aggregation: bacterial cells are connected and bridged by eDNA and EPS; (2) accumulation: a core of EPS-enmeshed bacterial cells is formed to provide a supporting framework; (3) maturation: bacterial cells divide and accumulate with EPS and DNA evenly distributing in the biofilm (Fig. 7). The interaction between eDNA and EPS plays vital role in the exploration of 3D biofilm architecture construction. In addition, the eDNA-EPS interaction might increase the survival of *B. subtilis* SBE1 in different environment by allowing eDNA from other microbial species as a scaffold on which to grow its own communities.

Supplementary Information

Supplementary Information contains (1) additional details on the materials and methods; (2) a table of strains, plasmids, and primers used in this study; (3)a figure of phylogenetic tree and gene family analysis of *B. subtilis* species; (4) a figure of total carbohydrate content of EPS produced by *B. subtilis* SBE1 and its EPS mutant (Δ*eps*G); (5) a figure of structural arrangement of bacteria during biofilm development of *B. subtilis* SBE1 and its EPS mutant (ΔepsG); (6) a figure of isothermal titration calorimetry measurement to determine the interaction of EPS and genomic DNA

Declarations

Acknowledgments

We thank Zhe Hu for the help in technical matters of SIM.

Authors' contributions

N. P. conceived the experimental strategy, conducted experiments, acquired data, analyzed data and wrote the manuscript. P. C. acquired funding, conceived the experimental strategy, wrote the manuscript. M. M wrote the manuscript. Y. C. W and C. H. G analyzed data. Q. Y. H wrote the manuscript. All authors have read and approved the manuscript.

Funding

This work was supported by the National Basic Research Program of China (2016YFD0800206), National Natural Science Foundation of China (41877029) and the Fundamental Research Funds for the Central Universities (2662017JC008).

Availability of data and materials

The datasets analyzed during the current study are available from the corresponding author upon reasonable request.

Ethics approval and consent to participate

No human/animal experiment is involved in this study.

Competing interests

The authors declare that there are no conflicts of interest.

References

[1] M. Ghannoum and G.A. O'Toole. Microbial Biofilms, Washington, DC: *ASM Press* (2004).

[2] P.S. Stewart and M.J. Franklin. Physiological Heterogeneity in Biofilms. *Nat. Rev. Microbiol.* 6 (2008) 199-210.

[3] D. López, R. Kolter. Functional microdomains in bacterial membranes. *Genes Dev* 24 (2010) 1893–1902.

[4] S.S. Branda, Vik Å, L. Friedman and R. Kolter. Biofilms: the matrix revisited. *Trends Microbiol* 13(1) (2005) 0-26.

[5] H-C. Flemming, J. Wingender. The biofilm matrix. *Nat. Rev. Microbiol.* 8 (2010) 623–633.

[6] C.B. Whitchurch, T. Tolker-Nielsen, P.C. Ragas, J.S. Mattick. Extracellular DNA required for bacterial biofilm formation. *Science* 295 (2002) 1487.

[7] D.M. Dominiak, J.L. Nielsen, and P.H. Nielsen. Extracellular DNA is abundant and important for microcolony strength in mixed microbial biofilms. *Environ. Microbiol.* 13 (2011) 710–721.

[8] Finkel, S.E., and Kolter, R. DNA as a nutrient: novel role for bacterial competence gene homologs. *J Bacteriol* 183 (2001) 6288–6293.

[9] S. Molin, T. Tolker-Nielsen. Gene transfer occurs with enhanced efficiency in biofilms and induces enhanced stabilization of the biofilm structure. Curr. Opin. Biotechnol. 14 (2003) 255–261.

[10] Z. Qin, Y. Ou, L. Yang, Y. Zhu, T. Tolker-Nielsen, S. Molin, D. Qu. Role of autolysin-mediated DNA release in biofilm formation of *Staphylococcus epidermidis. Microbiology* 153 (2007) 2083–2092.

[11] L. Hall-stoodley, L. Nistico, K. Sambanthamoorthy, B. Dice, D. Nguyen, J.W. Mershon, C. Johnson, F.Z. Hu, P. Stoodley, G.D. Ehrlich and J.C. Post. Characterization of biofilm matrix, degradation by DNase treatment and evidence of capsule downregulation in *Streptococcus pneumoniae* clinical isolates. *BMC Microbiol.* 8 (2008) 173.

[12] A. Seper, V.H.I. Fengler, S. Roier, H. Wolinski, S.D. Kohlwein, A.L. Bishop, A. Camilli, J. Reidl and S. Schild. Extracellular nucleases and extracellular DNA play important roles in *Vibrio cholerae* biofilm formation. *Mol. Microbiol.* 82 (2011) 1015–1037.

[13] L. Ma, M. Conover, H. Lu, M.R. Parsek, K. Bayles and D.J. Wozniak. Assembly and development of the *Pseudomonas aeruginosa* biofilm matrix. *PLoS Pathog* 5 (2009) e1000354.

[14] Sutherland, I. W. in Comprehensive Glycoscience Vol. 2 (ed. Kamerling, J. P.) 521–558 (Elsevier, Doordrecht, 2007).

[15] J. Xiao, M.I. Klein, M.L. Falsetta, B. Lu, C.M. Delahunty, J.R. Yates, A. Heydorn, H. Koo. The exopolysaccharide matrix modulates the interaction between 3D architecture and virulence of a mixed-species oral biofilm. *PLoS Pathog* 8 (2012) e1002623.

[16] S. Liao, M.I. Klein, K.P. Heim, Y. Fan, J.P. Bitoun, S.J. Ahn, R.A. Burne, H. Koo, L.J. Brady, Z. Wen. *Streptococcus mutans* extracellular DNA is upregulated during growth in biofilms, actively released via membrane vesicles, and influenced by components of the protein secretion machinery. *J Bacteriol* 196 (2014) 2355-2366.

[17] S. Wang, X. Liu, L. Zhang, Y. Guo, S. Yu, D.J. Wozniak, L.Z. Ma. The exopolysaccharide Psl–eDNA interaction enables the formation of a biofilm skeleton in *Pseudomonas aeruginosa. Environ. Microbiol. Rep.* 7(2) (2015) 330-340.

[18] H.P. Bais, R. Fall, J.M. Vivanco. Biocontrol of *Bacillus subtilis* against infection of Arabidopsis Roots by *Pseudomonas syringae* is facilitated by biofilm formation and surfactin production. *Plant Physio* 134(1) (2004) 307-319.

[19] T. Stein, S. Dusterhus, A. Stroh, K.D. Entian. Subtilosin production by two *Bacillus subtilis* subspecies and variance of the *sbo-alb* cluster. *Appl Environ Microbiol* 70 (2004) 2349–2353.

[20] R.A. Butcher, F.C. Schroeder, M.A. Fischbach, P.D. Straightt, R. Kolter, C.T. Walsh, J. Clardy. The identification of bacillaene, the product of the PksX megacomplex in *Bacillus subtilis*. *Proc. Natl. Acad. Sci. U. S. A.* 104 (2007) 1506–1509.

[21] K. Nagorska, M. Bikowski, M. Obuchowskji. Multicellular behaviour and production of a wide variety of toxic substances support usage of *Bacillus subtilis* as a powerful biocontrol agent. *Acta Biochim Pol* 54 (2007) 495–508.

[22] M. Ongena, E. Jourdan, A. Adam, M. Paquot, A. Brans, B. Joris, J.L. Arpigny, P. Thonart. Surfactin and fengycin lipopeptides of *Bacillus subtilis* as elicitors of induced systemic resistance in plants. *Environ. Microbiol.* 9 (2007) 1084–1090.

[23] M. Ongena, P. Jacques. *Bacillus* lipopeptides: versatile weapons for plant disease biocontrol. *Trends Microbiol* 16 (2008) 115–125.

[24] Y. Chen, S. Cao, Y. Chai, J. Clardy, R. Kolter, J.H. Guo, R. Losick. A *Bacillus subtilis* sensor kinase involved in triggering biofilm formation on the roots of tomato plants. *Mol Microbiol* 85 (2012) 418–430.

[25] Y. Chen, F. Yan, Y. Chai, H. Liu, R. Kolter, R. Losick, J.H. Guo. Biocontrol of tomato wilt disease by *Bacillus subtilis* isolates from natural environments depends on conserved genes mediating biofilm formation. *Environ Microbiol* 15 (2013) 848–864.

[26] P.B. Beauregard, Y. Chai, H. Vlamakis, R. Losick, R. Kolter. *Bacillus subtilis* biofilm induction by plant polysaccharides. *Proc Natl Acad Sci U S A* 110 (2013) E1621–1630.

[27] S.S. Branda, F. Chu, D.B. Kearns, R. Losick, R. Kolter. A major protein component of the *Bacillus subtilis* biofilm matrix. *Mol Microbiol* 59 (2006) 1229–1238.

[28] R.P. Sinha, V.N. Iyer. Competence for genetic transformation and the release of DNA from *Bacillus subtilis*[J]. *Biochimica et Biophysica Acta (BBA)-Nucleic Acids and Protein Synthesis* 232(1) (1971) 61-71.

[29] D. López, H. Vlamakis, R. Losick, and R. Kolter. Cannibalism enhances biofilm development in *Bacillus subtilis*. *Mol. Microbiol.* 74 (2009) 609–618.

[30] W.D. Crabb, U.N. Streips, and R.J. Doyle. Selective enrichment for genetic markers in DNA released by competent cultures of *Bacillus subtilis*. *Mol. Gen. Genet.* 155 (1977) 179–183.

[31] A.L. Ibáñez de Aldecoa, O. Zafra, & J.E. González-Pastor. Mechanisms and regulation of extracellular DNA release and its biological roles in microbial communities. *Front Microbiol* 8 (2017) 1390.

[32] O. Zafra, María Lamprecht-Grandío, C. González de Figueras, & J. E. González-Pastor. Extracellular DNA release by undomesticated *Bacillus subtilis* is regulated by early competence. *PLOS ONE*, 7 (2012).

[33] A. Wach. PCR-synthesis of marker cassettes with long flanking homology regions for gene disruptions in *S. cerevisiae*. *Yeast* 12(3) (1996) 259-265.

[34] B.M. Coffey, & G.G. Anderson. Biofilm formation in the 96-well microtiter plate. In Pseudomonas Methods and Protocols (pp. 631-641). *Humana Press*, New York, NY (2014).

[35] E.S. Gloag, L. Turnbull, A. Huang, P. Vallotton, H. Wang, L.M. Nolan & L.G. Monahan. Self-organization of bacterial biofilms is facilitated by extracellular DNA. *Proceedings of the National Academy of Sciences* 110(28) (2013) 11541-11546.

[36] W. Ma, D. Peng, S.L. Walker, B. Cao, C.H. Gao, & Q. Huang, C. Peng. *Bacillus subtilis* biofilm development in the presence of soil clay minerals and iron oxides. *npj Biofilms and Microbiomes*, 3 (2017) 4.

[37] M. Okshevsky, & R.L. Meyer. Evaluation of fluorescent stains for visualizing extracellular DNA in biofilms. *J Microbiol Meth* 105 (2014) 102-104.

[38] G.H. Yu, Z. Tang, Y.C. Xu, & Q.R. Shen. Multiple fluorescence labeling and two dimensional FTIR$-^{13}$C NMR heterospectral correlation spectroscopy to characterize extracellular polymeric substances in biofilms produced during composting. *Environmental Science & Technology*, 45 (2011) 9224-9231.

[39] J. Xiao, H. Koo. Structural organization and dynamics of exopolysaccharide matrix and microcolonies formation by *Streptococcus mutans* in biofilms[J]. *J. Appl. Microbiol.* 108 (2010) 2103-2113.

[40] W.S. Rasband. ImageJ. US National Institutes of Health, Bethesda, MD, U.S.A (1997–2006).

[41] B. Ni, Z. Huang, Z. Fan, C.Y. Jiang, and S.J. Liu. *Comamonas testosteroni* uses a chemoreceptor for tricarboxylic acid cycle intermediates to trigger chemotactic responses towards aromatic compounds. *Mol Microbiol* 90 (2013) 813–823.

[42] L. Tang, A. Schramm, T.R. Neu, N.P. Revsbech, R.L. Meyer. Extracellular DNA in adhesion and biofilm formation of four environmental isolates: a quantitative study. *FEMS Microbiol Ecol* 86 (2013) 394–403.

[43] S. Vilain, J.M. Pretorius, J. Theron, V.S. Brözel. DNA as an adhesin: *Bacillus cereus* requires extracellular DNA to form biofilms. *Appl. Environ. Microbiol.* 75 (2009) 2861–8.

[44] M. Lappann, H. Claus, T. van Alen, M. Harmsen, J. Elias, S. Molin, U. Vogel. A dual role of extracellular DNA during biofilm formation of *Neisseria meningitidis*. *Mol. Microbiol.* 75 (2010) 1355–1371.

[45] L. Hobley, C. Harkins, C.E. Macphee, N.R. Stanleywall. Giving structure to the biofilm matrix: an overview of individual strategies and emerging common themes. *FEMS Microbiol. Rev.* 39 (2015) 649-69.

[46] M. Harmsen, M. Lappann, S. Knøchel, S. Molin. Role of extracellular DNA during biofilm formation by *Listeria monocytogenes*. *Appl Environ Microbiol* 76 (2010) 2271–2279.

[47] E. Manders, J. Stap, G. Brakenhoff, R. van Driel & J. Aten. Dynamics of three-dimensional replication patterns during the Sphase, analysed by double labelling of DNA and confocal microscopy. *J. Cell Sci.* 103 (1992) 857–862.

[48] S. Bolte, & F.P. Cordelieres. A guided tour into subcellular colocalization analysis in light microscopy. *J. Microsc.* 224 (2006) 213-232.

[49] S.S. Branda, J.E. González-Pastor, S. Ben-Yehuda, R. Losick, R. Kolter. Fruiting body formation in *Bacillus subtilis*. *Proc Natl Acad Sci U S A* 98 (2001) 11621-11626.

[50] D.B. Kearns, F. Chu, S.S. Branda, R. Kolter, R. Losick. A master regulator for biofilm formation by *Bacillus subtilis*. *Mol Microbiol* 55 (2005) 739–749.

[51] S.B. Guttenplan, K.M. Blair, D.B. Kearns. The EpsE flagellar clutch is bifunctional and synergizes with EPS biosynthesis to promote *Bacillus subtilis* biofilm formation[J]. *PLoS Genet* 6 (2010) e1001243.

[52] M. Serrano, R. Zilhão, E. Ricca, A.J. Ozin, C.P. Moran, & A.O.A. Henriques. *Bacillus subtilis* secreted protein with a role in endospore coat assembly and function. *J. Bacteriol.* 181 (1999) 3632-3643.

[53] S.S. Branda, J.E. González-Pastor, E. Dervyn, S.D. Ehrlich, R. Losick, & R. Kolter. Genes involved in formation of structured multicellular communities by *Bacillus subtilis*. *J. Bacteriol.* 186 (2004) 3970-3979.

[54] M.C. Castillo Pedraza, T.F. Novais, R.C. Faustoferri, R.G. Quivey, A. Terekhov, B.R. Hamaker, & M.I. Klein. Extracellular DNA and lipoteichoic acids interact with exopolysaccharides in the extracellular matrix of *Streptococcus mutans* biofilms. *Biofouling* 33 (2017) 722–740.

[55] A. Gries, R. Prassl, S. Fukuoka, M. Rossle, Y. Kaconis, L. Heinbockel, T. Gutsmann, K. Brandenburg. Biophysical analysis of the interaction of the serum protein human beta2GPI with bacterial lipopolysaccharide. *FEBS Open Bio* 4 (2014) 432–440.

Figures
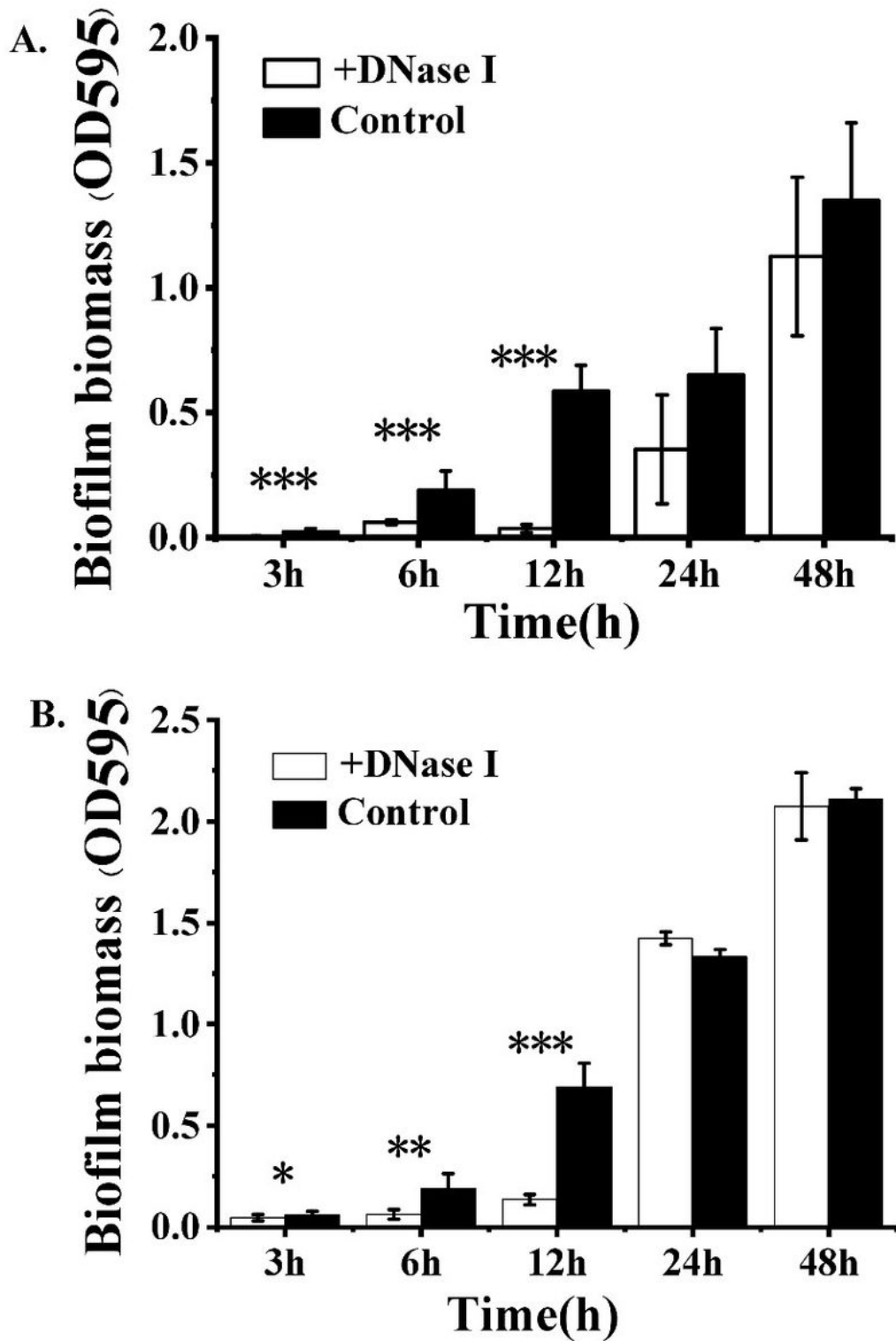
Figure 1

Effects of DNase I treatment on the early stages of statically grown biofilms of B. subtilis SBE1. B. subtilis was incubated with (white bars) or without (black bars) DNase I in the growth medium and after 3, 6, 12 h (a) and 24, 48 h (b) biofilm was quantified using a crystal violet assay. The bars are means of five replicates, and the error bars represent standard deviations. *P < 0.05, **P < 0.01, ***P < 0.001 for comparisons of data obtained in the absence of DNase I and in the presence of DNase I.
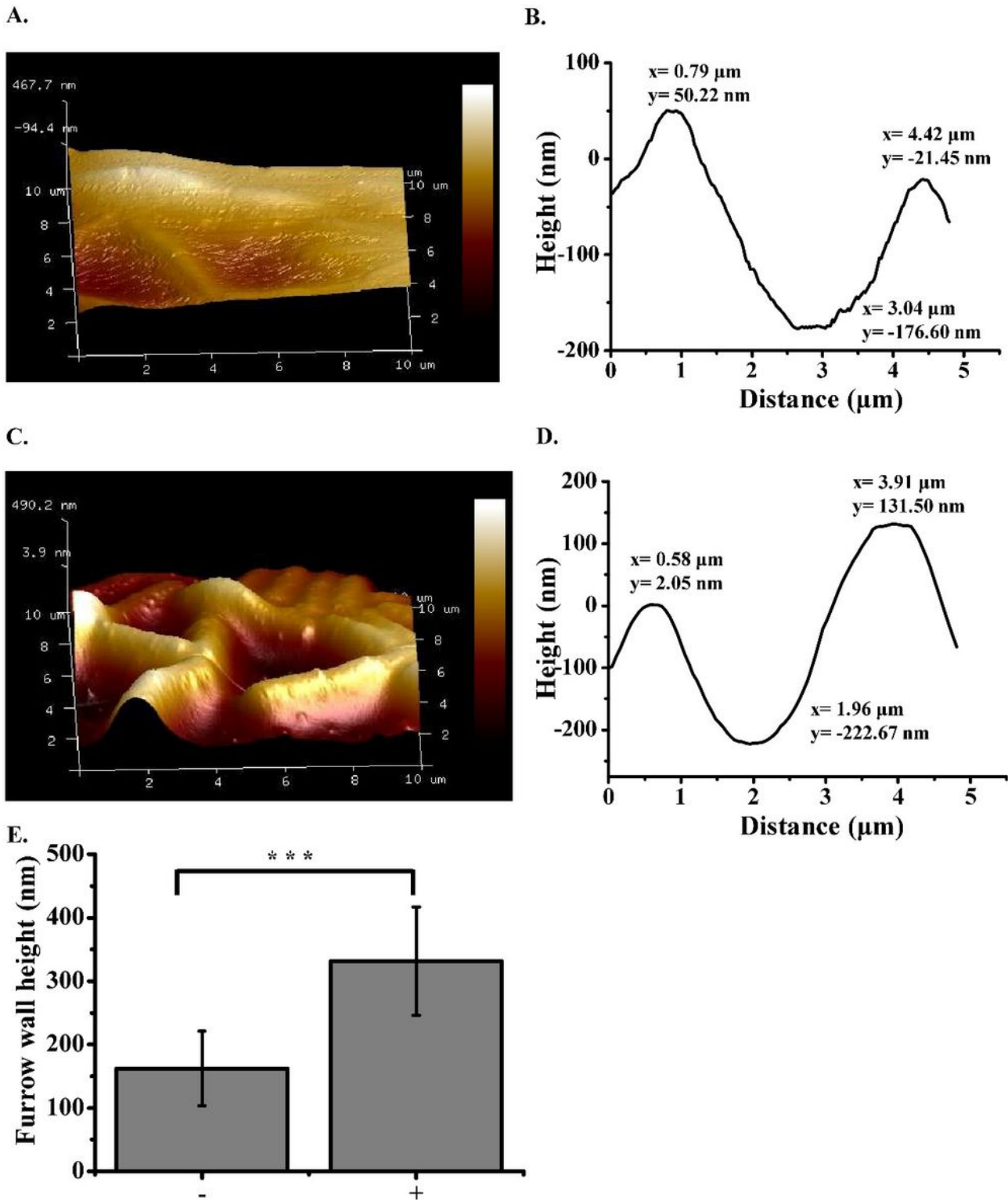
Figure 2

. AFM surface profiles of biofilms (12 h). 3D AFM images of biofilms cultured in the absence (A) and presence of DNase I (C). Scale is a relative color scale. A is scaled to 467.7 nm, and C is scaled to 490.2 nm. Measurements were taken between cells to generate a depth profile as shown in B and D. The y-axis scale is different for B and D. (E) Depths of furrows between cells from biofilms cultured in the absence (-,

Figure 3

Dynamics of morphogenesis, 3D architecture development and microbial population shifts of B. subtilis SBE1 biofilms. The biofilms stained with TOTO-1 for eDNA (green) and SYTO 60 for bacteria (red). Representative 3D rendering images of B. subtilis SBE1 biofilms at 12 h (A), 24 h (B) and 48 h (C). The

eDNA channel is depicted in green, while the cells are depicted in red. At the upper left of each panel, the two channels are displayed separately, while the merged image is displayed at the bottom right. A magnified (close-up) view of each small box depicted in the merged image is positioned in the upper right corner of each panel.

B.
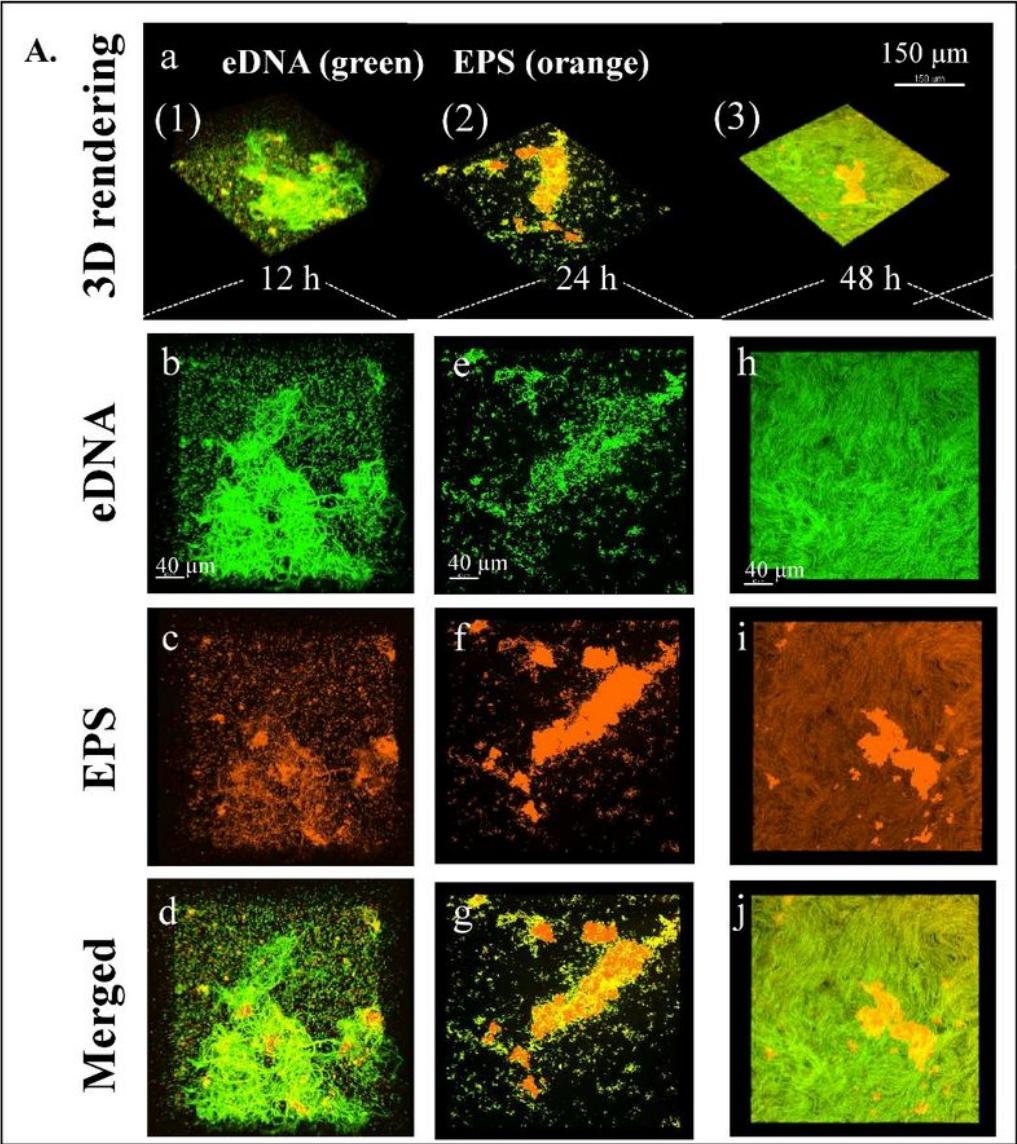
Biomass (μm³/μm²)	12 h	24 h	48 h
eDNA	1.29±0.21	0.89±0.26	1.96±0.14
EPS	1.09±0.12	1.80±0.22	1.65±0.49

Figure 4

Structural arrangement between EPS and eDNA during biofilm development of B. subtilis SBE1 and its EPS mutant (ΔepsG). (A) Representative 3D renderings of B. subtilis SBE1 biofilms at 12, 24 and 48 h: (a) shows the dynamic evolution of biofilms over time. Panel (b-J) show cross sectional images of selected area for close-up views of structural organization of EPS (orange) and eDNA (green) during the development of biofilm matrix complex. (B) The biomass values of EPS and eDNA in the biofilms were calculated using Imaris. The data shown are mean values ± SD (n = 3).
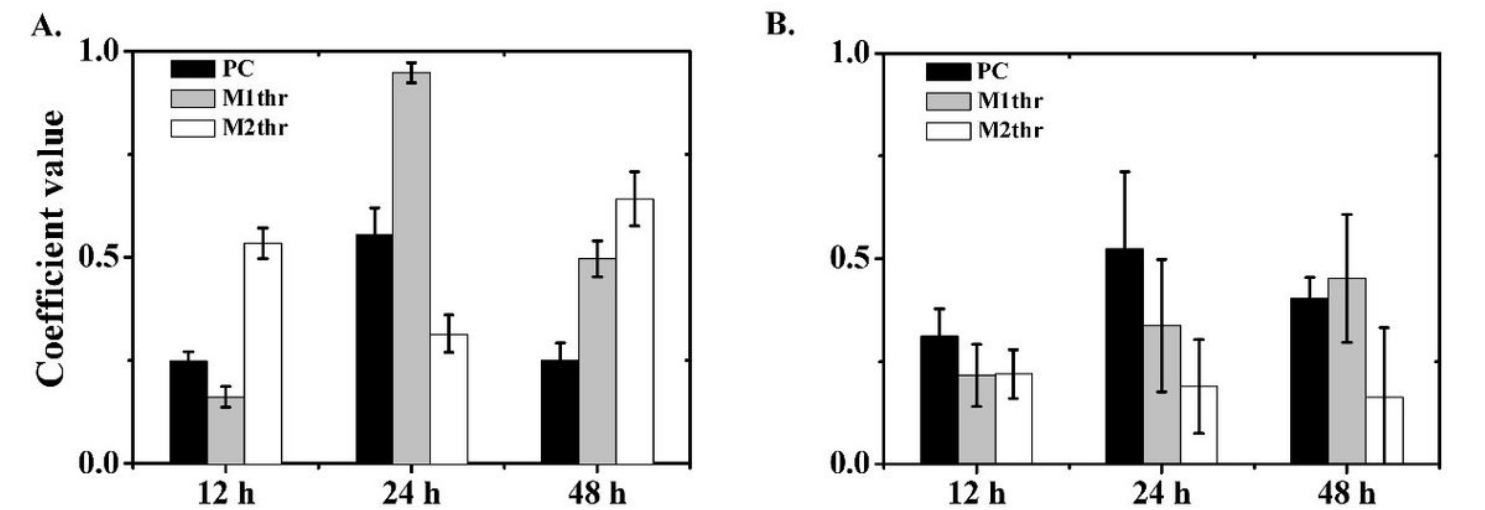
Figure 5

The analysis of eDNA-EPS colocalization coefficients in B. subtilis SBE1 (A) and its EPS mutant (ΔepsG) (B) biofilms. Columns showed the eDNA-EPS colocalization coefficients analyzed from seven images by three methods: Pearson's correlation coefficient (PC), the thresholded Mander's tM1 (M1thr) representing fraction of eDNA overlapping EPS, and tM2 (M2thr) representing fraction of EPS overlapping eDNA.

A.

B.
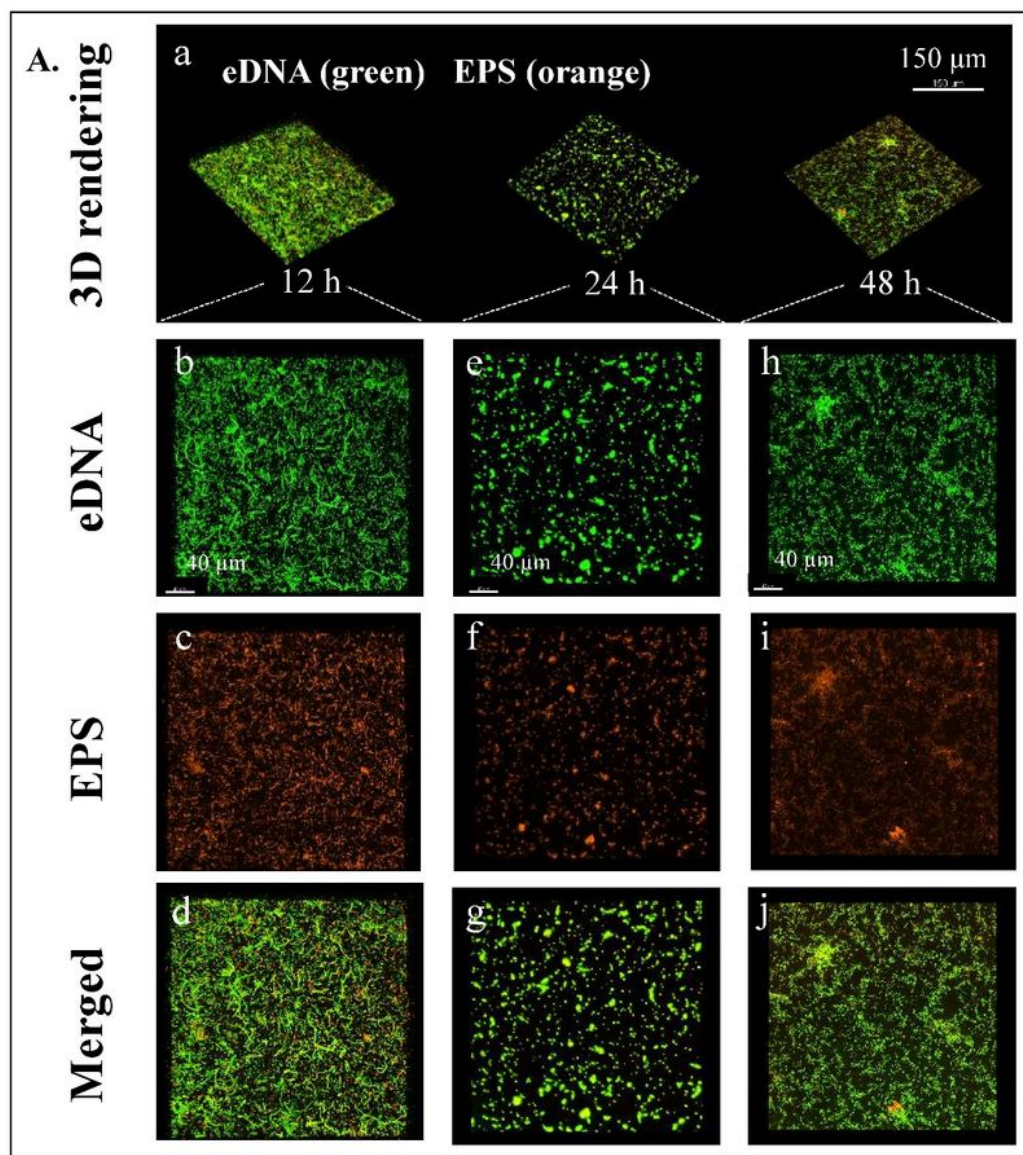
Biomass (μm³/μm²)	12 h	24 h	48 h
eDNA	0.73±0.11	0.75±0.12	0.77±0.03
EPS	0.74±0.03	0.81±0.14	0.76±0.06

Figure 6

Structural arrangement between EPS and eDNA during biofilm development of EPS mutant (ΔepsG). (A) Representative 3D renderings of B. subtilis SBE1 biofilms at 12, 24 and 48 h: (a) shows the dynamic evolution of biofilms over time. Panel (b-J) show cross sectional images of selected area for close-up views of structural organization of EPS (orange) and eDNA (green) during the development of biofilm

matrix complex. (B) The biomass values of EPS and eDNA in the biofilms were calculated using Imaris. The data shown are mean values ± SD (n = 3).
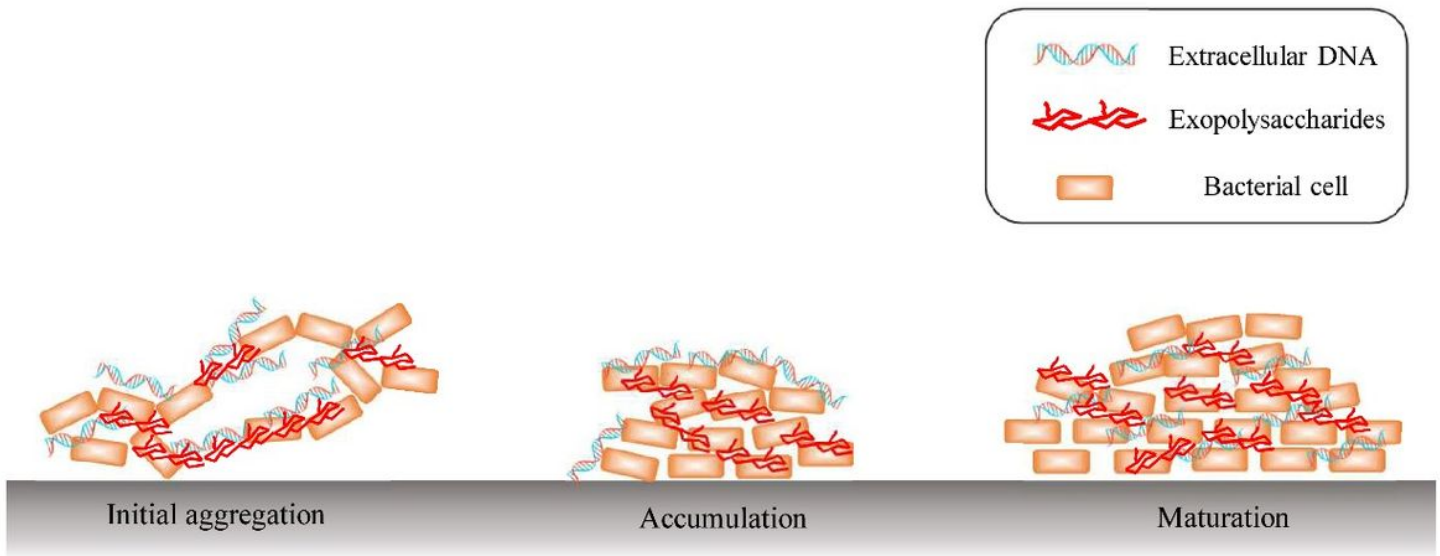
Figure 7

Proposed model for how eDNA-EPS interaction modulates 3D architecture of B. subtilis SBE1 biofilm. Complex 3D biofilm forms in the following sequence: (1) initial aggregation: bacterial cells were connected and bridged by eDNA and EPS; (2) accumulation: a core of EPS-enmeshed bacterial cells that provides a supporting framework; (3) maturation: bacterial cells divide and accumulate with EPS and DNA evenly distributed in the biofilms.